Journal of Sound and Vibration (2000) **238**(3), 389–399
doi:10.1006/jsvi.2000.3104, available online at http://www.idealibrary.com on IDEAL®

SPURIOUS RESONANCES IN NUMERICAL TIME INTEGRATION METHODS FOR LINEAR DYNAMICS

V. Cannillo and M. Mancuso

Dipartimento di Scienze dell'Ingegneria, Università degli Studi di Modena e Reggio Emilia, via Campi 213/b, 41100 Modena, Italy

(*Received* 19 *January* 2000, *and in final form* 29 *March* 2000)

This paper deals with the accuracy of time integration methods for linear dynamics when applied near the resonance condition. An approach for the analysis is considered which allows spurious resonance conditions to be detected. The analysis of Newmark methods shows the existence of such conditions which can adversely affect the quality of numerical computations. As an alternative, a higher order algorithm, which can be viewed as a generalization of the trapezoidal rule, is investigated. The analysis reveals that the spurious disturbance near the resonance condition is greatly reduced. The reported numerical tests confirm the theoretical predictions and demonstrate that high-quality simulations can be obtained by means of higher order algorithms.

1. INTRODUCTION

Numerical time integration algorithms for linear dynamics are usually analyzed with reference to the homogeneous part of the solution [1, 2]. In this way, the accuracy analysis is greatly simplified and useful indications about the error evolution can be obtained. However, a complete accuracy analysis should take into account the part of the solution associated with the external load. Only a few studies on the algorithms behaviour with a forcing term are available (see, for example, references [3–5]). In these cases the accuracy analysis aims to determine an adequate approximation of the external loads in order to retain the same order of accuracy of the homogeneous solution. This analysis procedure is focused only on the error for small time steps and therefore no information is made available regarding the behaviour with relatively large time steps.

A different approach to the accuracy analysis of the forcing term was introduced by Preumont [6]. The time integration operators are treated as digital recursive filters and the transfer functions of the discretized equations are derived. The comparison between the numerical and the exact transfer functions gives a more complete picture of the algorithm behaviour and allows spurious resonance conditions to be detected. In particular, this procedure applied to Newmark methods shows that in correspondence to the resonance frequency the algorithms are inaccurate, i.e., a spurious peak in the ratio of the exact to the numerical transfer function.

In recent years, extensive research has been conducted on higher order methods (see, for example, the survey given by Fung [7, 8]). The main advantage of these methods is the low rate of error growth, which is a particularly advantageous feature in long-term simulations. In this paper, a fourth order algorithms derived from the postintegration technique [9] is considered and an analysis based on the approach introduced by Preumont is performed.

0022-460X/00/480389 + 11 $35.00/0

This algorithm shows a remarkable improvement over Newmark methods near the resonance condition, where the spurious peak is significantly reduced. An experimental evaluation of the algorithm is included, which confirms the theoretical analysis. It is shown that the error in the simulations based on the higher order method is more than two orders of magnitude lower than that obtained with the trapezoidal rule.

An outline of the paper follows. In section 2, the initial-value problem is formulated. In section 3, the time integration methods considered here are described. In section 4, an analysis of the algorithms is given. Numerical tests are reported in section 5 and conclusions are drawn in section 6.

2. THE INITIAL-VALUE PROBLEM

The equations of motion of linear multi-degree-of-freedom systems may be written as follows:

$$\mathbf{M}\ddot{\mathbf{u}}(t) + \mathbf{C}\dot{\mathbf{u}}(t) + \mathbf{K}\mathbf{u}(t) = \mathbf{f}(t), \quad t \in (0, t_f], \tag{1}$$

where superposed dots denote differentiation with respect to time t, $\mathbf{M}$ is the mass matrix, $\mathbf{C}$ is the damping matrix, $\mathbf{K}$ is the stiffness matrix, $\mathbf{f}$ is the prescribed load vector and $\mathbf{u}$ is the unknown displacement vector. The initial conditions are given as

$$\mathbf{u}|_0 = \mathbf{u}_0, \qquad \dot{\mathbf{u}}|_0 = \mathbf{v}_0, \tag{2, 3}$$

where $\mathbf{u}_0$ and $\mathbf{v}_0$ are the prescribed initial displacement and velocity vectors. The matrices $\mathbf{M}$, $\mathbf{C}$ and $\mathbf{K}$ are symmetric, $\mathbf{M}$ is positive-definite, $\mathbf{C}$ and $\mathbf{K}$ are positive-semidefinite. Under the hypothesis of proportional damping, the modal decomposition procedure (see reference [1] for details) can be used to decouple the initial-value problem defined by equations (1)–(3). The typical modal initial-value problem takes the form

$$\ddot{u}(t) + 2\xi\omega\dot{u}(t) + \omega^2 u(t) = f(t), \quad t \in (0, t_f], \tag{4}$$

$$u(0) = u_0, \qquad \dot{u}(0) = v_0, \tag{5, 6}$$

where the real non-negative parameter ω represents a natural frequency of the system and ξ is the damping ratio. In the analysis of numerical methods for the solution of equations (1)–(3), for simplicity the undamped case is considered ($\xi = 0$). Assuming that the forcing term can be expanded in Fourier series and invoking the superposition principle [10], it is sufficient to consider a generic sinusoidal component. Setting $f(t) = e^{ivt}$, the exact response in the mode corresponding to the frequency ω is given by

$$u(t) = u_h(t) + u_p(t), \tag{7}$$

where

$$u_h(t) = u_0 \cos(\omega t) + \frac{v_0}{\omega} \sin(\omega t) \tag{8}$$

is the homogeneous solution and

$$u_p(t) = \frac{-\omega \cos(vt) + \omega \cos(\omega t) - i\omega \sin(vt) + iv \sin(\omega t)}{\omega(v^2 - \omega^2)} \tag{9}$$

is the particular solution.

3. THE TIME INTEGRATION METHODS

Let $0 = t_0 < t_1 < \cdots < t_N = t_f$ be a partition of the time domain and let $\Delta t = t_{n+1} - t_n$ be the step size. The numerical approximations to $u(t_n)$ and $\dot{u}(t_n)$ are denoted by u_n and v_n respectively. Assuming that the numerical solution at $t = t_n$ is known from the $(n-1)$th time step, one-step time integration algorithms can be put in the form of a time advance scheme

$$\mathbf{y}_{n+1} = \mathbf{A}\mathbf{y}_n + \mathbf{L}_n, \quad n = 0, \ldots, N-1, \tag{10}$$

where $\mathbf{y}_n^{\mathrm{T}} = [u_n, v_n]$, $\mathbf{A}$ is the amplification matrix, $\mathbf{L}_n$ is the load vector, and the starting value $\mathbf{y}_0$ is given by equations (5) and (6). The load vector can be written as

$$\mathbf{L}_n = \mathbf{B}\mathbf{r}_n, \tag{11}$$

where the vector $\mathbf{r}_n$ collects the evaluations of the forcing term at some given sampling points and $\mathbf{B}$ is a matrix which does not depend on the forcing term. For example, in the case of Newmark methods

$$\mathbf{A} = \frac{1}{d}\begin{bmatrix} \frac{1}{2}(2 - \Omega^2 + 2\Omega^2\beta) & \Delta t \\ -\Omega^2(-\gamma\Omega^2 + 2 + 2\beta\Omega^2)/(2\Delta t) & \gamma\Omega^2 + 1 + \Omega^2\beta \end{bmatrix}, \tag{12}$$

$$\mathbf{B} = \frac{1}{d}\begin{bmatrix} -\frac{1}{2}\Delta t^2(-1 + 2\beta) & \Delta t^2\beta \\ \frac{1}{2}\Delta t(-\gamma\Omega^2 + 2 + 2\beta\Omega^2 - 2\gamma) & \gamma\Delta t \end{bmatrix}, \tag{13}$$

$$\mathbf{r}_n^{\mathrm{T}} = [f_n, f_{n+1}], \tag{14}$$

where $d = 1 + \beta\Omega^2$ and $\Omega = \omega\Delta t$.

The postintegration technique [9] is based on expressions of the velocity and the displacement which are both obtained by integrating the acceleration. At $t = t_{n+1}$

$$u_{n+1} = u_n + \Delta t v_n + D_n, \qquad v_{n+1} = v_n + V_n, \tag{15, 16}$$

where

$$D_n = \int_{t_n}^{t_{n+1}} (t_{n+1} - t)\ddot{u}(t)\,\mathrm{d}t, \qquad V_n = \int_{t_n}^{t_{n+1}} \ddot{u}(t)\,\mathrm{d}t. \tag{17, 18}$$

It is possible to formulate various families of methods based on equations (15)–(18). First, an approximate displacement $u(t)$ in $[t_n, t_{n+1}]$ is defined using the nodal values u_n, v_n, u_{n+1}, v_{n+1}. Next, the acceleration is obtained from the equation of motion (4), which in the case of $\xi = 0$ yields

$$\ddot{u}(t) = f(t) - \omega^2 u(t). \tag{19}$$

Substituting equation (19) into the integrals (17) and (18) gives

$$D_n = \int_{t_n}^{t_{n+1}} (t_{n+1} - t) f(t)\,\mathrm{d}t - \int_{t_n}^{t_{n+1}} (t_{n+1} - t)\omega^2 u(t)\,\mathrm{d}t, \tag{20}$$

$$V_n = \int_{t_n}^{t_{n+1}} f(t)\,\mathrm{d}t - \int_{t_n}^{t_{n+1}} \omega^2 u(t)\,\mathrm{d}t. \tag{21}$$

The time integration method is defined by the form of the approximate displacement and the quadrature rule used to evaluate the integrals in equations (20) and (21). Integrating equations (20) and (21) exactly with linear Hermite polynomials, the amplification matrix of the linear acceleration method is obtained. If a single-point quadrature rule is used, the Newmark methods are obtained with the parameters β and γ related to the position of the integration point and the integration weight. The trapezoidal rule is obtained setting the weight equal to 1 and placing the integration point in the middle of the interval.

Higher order methods can be obtained using higher order polynomials to represent the approximated displacement. The method considered here is based on a cubic Hermite polynomial. The Simpson rule is used to evaluate the integrals. The amplification matrix is

$$\mathbf{A} = \frac{1}{d}\begin{bmatrix} 144 - 60\Omega^2 + \Omega^4 & 12\Delta t(12 - \Omega^2) \\ 12\Omega^2(-12 + \Omega^2)/\Delta t & 144 - 60\Omega^2 + \Omega^4 \end{bmatrix}, \tag{22}$$

where $d = 144 + 12\Omega^2 + \Omega^4$ and $\Omega = \omega\Delta t$. The load term is defined by

$$\mathbf{B} = \frac{\Delta t}{d}\begin{bmatrix} -\Delta t(-24 + \Omega^2) & 48\Delta t & \Delta t\Omega^2 \\ -8(-3 + \Omega^2) & -8(-12 + \Omega^2) & 4(6 + \Omega^2) \end{bmatrix}, \tag{23}$$

$$\mathbf{r}_n^{\mathrm{T}} = [f_n, f_{n+1/2}, f_{n+1}], \tag{24}$$

where f_n, $f_{n+1/2}$, f_{n+1} are the evaluations of the forcing term at t_n, $t_n + \Delta t/2$ and t_{n+1} respectively. In the following, this method will be referred to as PI3 method.

4. ANALYSIS

Under the hypotheses of stability and consistency an algorithm is convergent [2], that is the numerical solution of the semidiscrete system approaches the exact one as $\Delta t \to 0$. The integration scheme is unconditionally stable if, and only if, the spectral radius of the amplification matrix $\mathbf{A}$ satisfies $\rho(\mathbf{A}) \leqslant 1$ for all Δt [1]. The local truncation error is defined as

$$\boldsymbol{\tau}(t_n) = \mathbf{y}(t_{n+1}) - \mathbf{A}\mathbf{y}(t_n) + \mathbf{L}_n,$$

where $\mathbf{y}^{\mathrm{T}}(t_n) = [u(t_n), v(t_n)]$. A time advance scheme is consistent if two positive constants C and k, not depending on Δt, exist, for which

$$\| \boldsymbol{\tau}(t_n) \| \leqslant C\Delta t^{k+1}.$$

4.1. ACCURACY OF THE HOMOGENEOUS SOLUTION

Besides the local truncation error, the following measures of accuracy are widely used in the analysis of time integration methods [2]: (1) the algorithmic damping ratio $\bar{\xi}$, abbreviated as adr, (2) the relative period error $\Omega/\bar{\Omega} - 1$, abbreviated as rpe.

Newmark methods with $\frac{1}{2} \leqslant \gamma \leqslant 2\beta$ are unconditionally stable and second order accurate for $\gamma = \frac{1}{2}$.

It can be easily shown that the algorithm PI3 described by equations (22) and (23) is unconditionally stable and the spectral radius is equal to 1 for all Δt. Table 1 shows the local truncation errors for the homogeneous part, the algorithmic damping ratio and the relative period error, thus indicating that the algorithm is fourth order accurate.

TABLE 1

PI3 method—measures of accuracy of the homogeneous solution

	Coefficient	Order
Displacement	$\frac{1}{720} v_0 \omega^4$	Δt^5
Velocity	$-\frac{1}{720} u_0 \omega^6$	Δt^5
adr	0	
rpe	$\frac{1}{720}$	Ω^4

TABLE 2

PI3 method—lte of the particular solution

	Coefficient	Order
Displacement	$-\frac{1}{720} \mathrm{i}\nu(\omega^2 + \nu^2)$	Δt^5
Velocity	$\frac{1}{720} \omega^2 \nu^2 - \frac{1}{2880} \nu^4 + \frac{1}{720} \omega^4$	Δt^5

4.2. ACCURACY OF THE PARTICULAR SOLUTION

Table 2 shows the local truncation error for the particular integral (in the case of exponential excitation $\mathrm{e}^{\mathrm{i}\nu t}$) for the PI3 method. It can be seen that the particular solution has the same order of accuracy of the homogeneous solution.

To get more insight into the accuracy of the loading term, it is useful to refer to the transfer function H_u^*. Considering the modal initial-value problem (equation (4)) with $\xi = 0$ and assuming that the forcing term is $\mathrm{e}^{\mathrm{i}\nu t}$, the transfer function has the well-known form [10]

$$H_u^* = \frac{1}{\omega^2 - \nu^2}. \tag{25}$$

Following Preumont [6], it is possible to obtain an expression for the transfer function of the time advance scheme (equation (10)), which can be compared with equation (25) and used to analyze the behaviour of the algorithm with regard to the response to a forcing term.

If it is assumed that the excitation has complex exponential form $f(t) = \mathrm{e}^{\mathrm{i}\nu t}$, at $t = t_n$, the solution can be written as

$$\begin{pmatrix} u_n \\ v_n \end{pmatrix} = \begin{pmatrix} H_u \\ H_v \end{pmatrix} \mathrm{e}^{\mathrm{i}\nu n \Delta t}, \tag{26}$$

where H_u and H_v are the transfer function for the numerical displacement and velocity. Using equations (10) and (26),

$$\begin{pmatrix} H_u \\ H_v \end{pmatrix} = [e^{iv\Delta t}\mathbf{I} - \mathbf{A}]^{-1}\mathbf{B}\mathbf{r} \tag{27}$$

is obtained where $\mathbf{I}$ is the identity matrix, $\mathbf{r}^T = [1, e^{iv\Delta t}]$ for the Newmark method and $\mathbf{r}^T = [1, e^{iv\Delta t/2}, e^{iv\Delta t}]$ for the PI3 algorithm.

The comparison of H_u and H_v with the exact forms H_u^* and $H_v^* = ivH_u^*$ gives the desired information about the behaviour of the algorithm with regard to the forcing term.

The ratio $|H_u|/|H_u^*|$ has been analyzed for the Newmark methods for various values of the parameters β and γ [6]. The same analysis of the ratio $|H_u|/|H_u^*|$ is performed here for the PI3 algorithm. In Figure 1 the trapezoidal rule and the PI3 method are compared assuming $\Omega/2\pi = 0{\cdot}2$. The ratio $|H_u|/|H_u^*|$ is plotted versus the ratio $\varepsilon = v/\omega$. It can be noted that a spurious peak (corresponding to a vertical asymptote of $|H_u|/|H_u^*|$) occurs near the resonance condition ($\varepsilon = 1$). As illustrated in the enlargement in Figure 2 the width of the disturbance in the PI3 algorithm is greatly reduced compared to the trapezoidal rule.

The value of ε corresponding to a spurious resonance can be derived as a function of Ω. With this aim, an expression for the ratio $|H_u|/|H_u^*|$ has been obtained, and values of ε corresponding to vertical asymptotes (i.e., spurious resonance conditions) have been sought. For both the Newmark method and the PI3 algorithm the numerator of $|H_u|/|H_u^*|$ is equal to zero only if $\varepsilon = 1$, while the denominator is zero for values of ε satisfying the following equations:

$$x^2(\Omega^4 + 12\Omega^2 + 144) + x(120\Omega^2 - 2\Omega^4 - 288) + \Omega^4 + 12\Omega^2 + 144 = 0, \tag{28}$$

$$x^2(\Omega^2 + 4) + x(2\Omega^2 - 8) + \Omega^2 + 4 = 0 \tag{29}$$

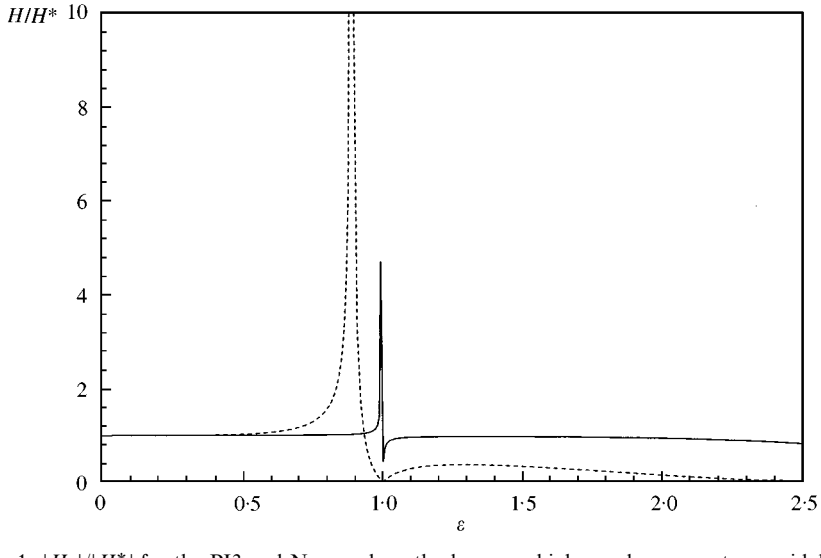

Figure 1. $|H_u|/|H_u^*|$ for the PI3 and Newmark methods: ____ higher order; _ _ _ _ trapezoidal rule.

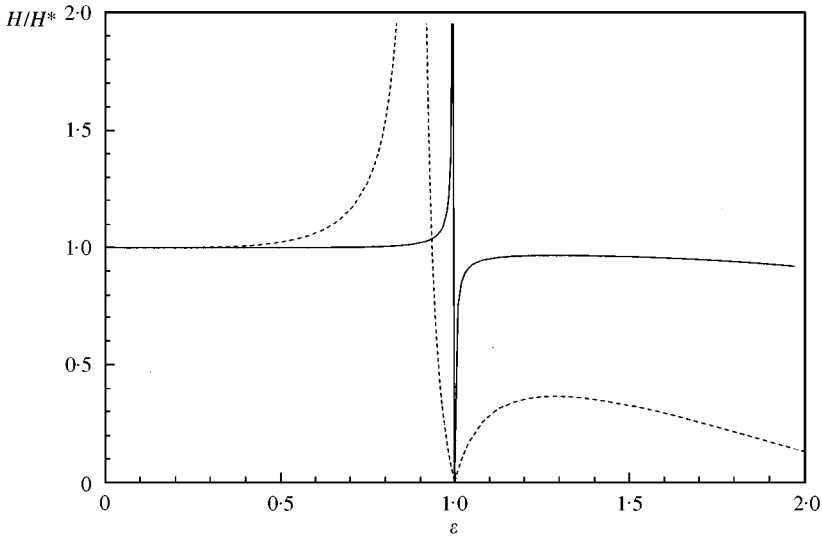

Figure 2. $|H_u|/|H_u^*|$ for the PI3 and Newmark methods: ____ higher order; - - - - trapezoidal rule.

for the PI3 algorithm and the trapezoidal rule, respectively, where $x = e^{i\Omega\varepsilon}$, $\Omega = \omega\Delta t$. Solving for x, an expression for ε can be obtained as a function of Ω, i.e.,

$$\varepsilon = \frac{1}{\Omega}\arctan(144\Omega - 12\Omega^3,\ 144 - 60\Omega^2 + \Omega^4) \tag{30}$$

for the PI3 algorithm and

$$\varepsilon = \frac{1}{\Omega}\arctan(4\Omega,\ -\Omega^2 + 4) \tag{31}$$

for the trapezoidal rule, where the two-argument function $\arctan(b, a)$ computes the principal value of the argument of the complex number $a + ib$ (so $-\pi < \arctan(b, a) \leqslant \pi$). Expanding $\varepsilon(\Omega)$ in Taylor series, one obtains

$$\varepsilon = 1 - \frac{1}{720}\Omega^4 + o(\Omega^5) \tag{32}$$

for the PI3 algorithm and

$$\varepsilon = 1 - \frac{1}{12}\Omega^2 + o(\Omega^3) \tag{33}$$

for the trapezoidal rule. These expressions show that the resonance condition occurs for $\varepsilon < 1$, for small values of $\omega\Delta t$. It should be noted that the shift in the position of the spurious resonance has the same order of the local truncation error.

5. NUMERICAL RESULTS

The numerical evaluation of the PI3 method and the comparison with the trapezoidal rule can be performed by considering a single-degree-of-freedom system excited by a sinusoidal force with v close to the frequency ω. The exact solution corresponding to

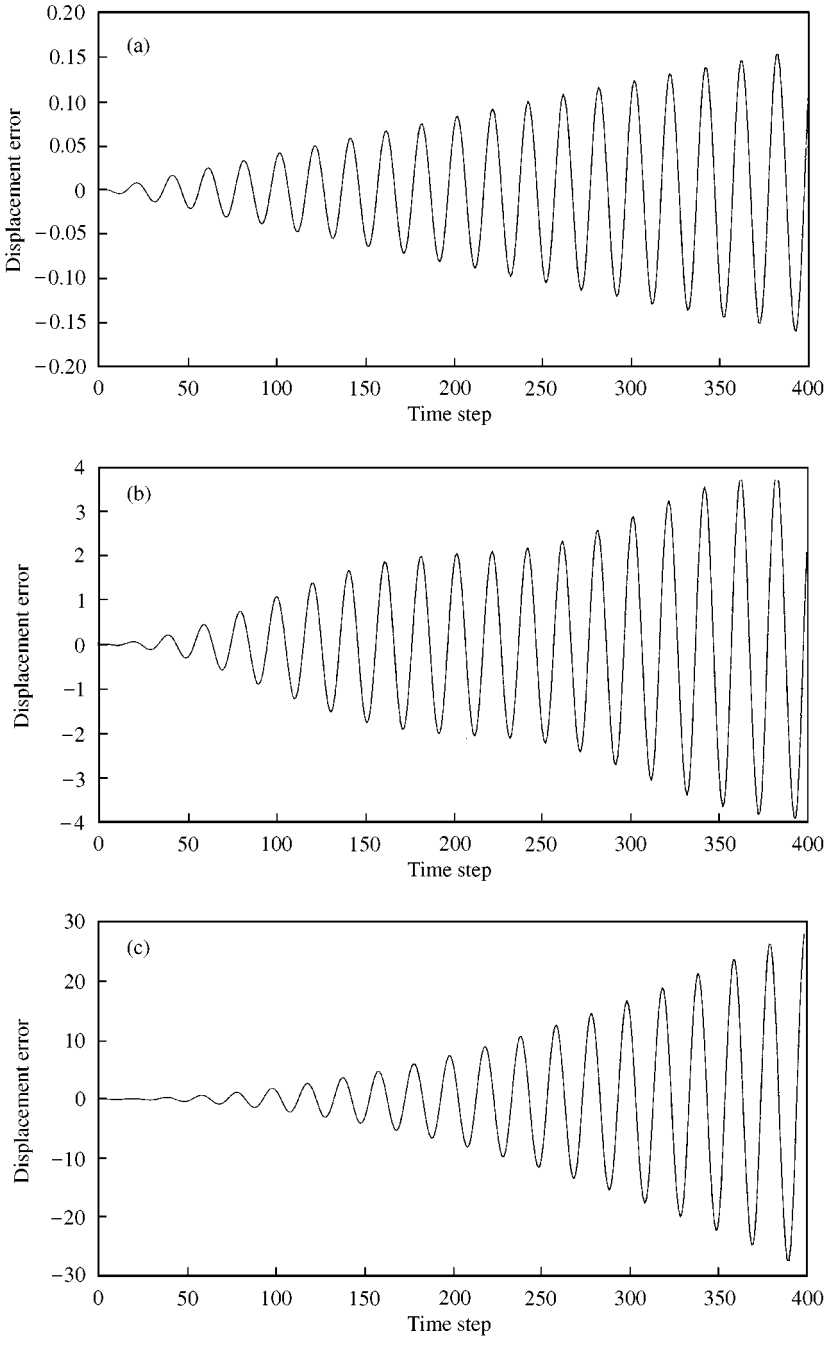

Figure 3. Time histories of the displacement error for the trapezoidal rule: (a) $\varepsilon = 0{\cdot}5$; (b) $\varepsilon = 0{\cdot}9$; (c) $\varepsilon = 0{\cdot}99$.

$u_0 = 0$, $v_0 = 0$ and $f(t) = \sin(vt)$ is

$$u(t) = \frac{-\omega \sin(vt) + v \sin(\omega t)}{\omega(v^2 - \omega^2)}. \tag{34}$$

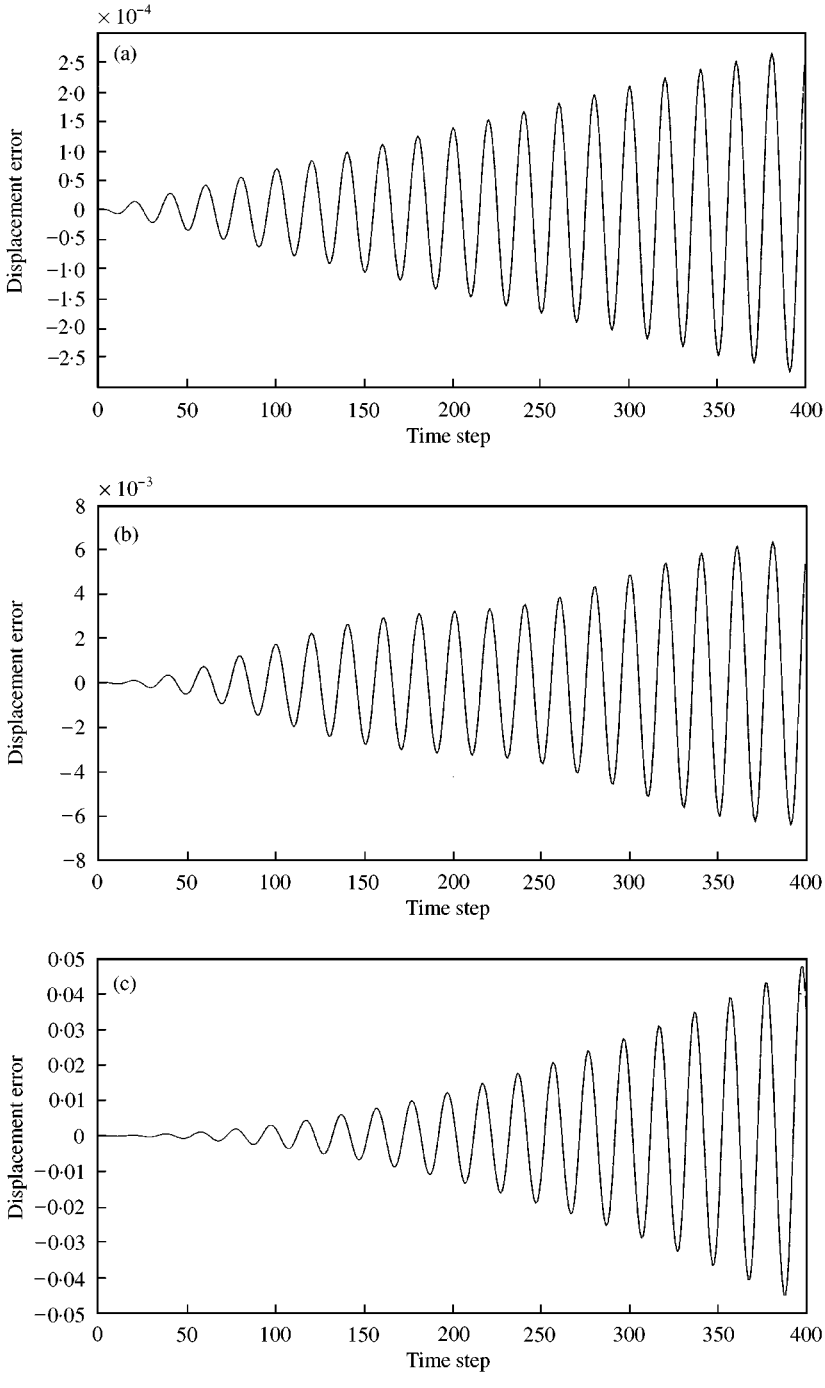

Figure 4. Time histories of the displacement error for the PI3 method: (a) $\varepsilon = 0{\cdot}5$; (b) $\varepsilon = 0{\cdot}9$; (c) $\varepsilon = 0{\cdot}99$.

The numerical simulations have been performed assuming $v = 1$ and $\Delta t = T/20$, where $T = 2\pi/\omega$ is the free vibration period of the system. The response up to $t_f = 20T$ is considered. Figure 3 shows some time histories of the displacement error (defined as the difference between the exact quantity and the numerical one) for the trapezoidal rule.

Different values of $\varepsilon = v/\omega$ are examined. The error accumulation for $\varepsilon = 0{\cdot}5$ is slow (Figure 3(a)), but it becomes faster as the resonance condition is approached ($\varepsilon = 0{\cdot}99$), as can be seen in Figure 3(c). The same tendency is observed in Figure 3(b) in the case of $\varepsilon = 0{\cdot}9$. The unsatisfactory behaviour of the Newmark methods near the resonance condition is evident. As regards the velocity error, the time evolutions are very similar to the corresponding displacement error and therefore are not shown.

Figure 4 shows the time histories of the displacement error for the PI3 method with the same values of ε used for the trapezoidal rule. The errors for $\varepsilon = 0{\cdot}5$ are small, as shown in Figure 4(a). However, even in the cases $\varepsilon = 0{\cdot}9$ and $0{\cdot}99$ the error accumulation is quite slow (Figures 4(b) and 4(c)): the errors are at least two orders of magnitude lower than those obtained by the trapezoidal rule.

In order to emphasize the improved performance of the PI3 method, the errors of the Newmark method and the PI3 method are plotted in Figure 5. Figure 6, which shows the velocity errors, confirms the higher accuracy of the PI3 method.

6. CONCLUSIONS

An approach for the accuracy analysis of time integration algorithms which takes into account the forcing term is described. This approach is based on comparison of the numerical and exact transfer functions. When applied to Newmark methods, this analysis reveals spurious resonance conditions that can compromise the solution. A higher order algorithm, formulated by means of the postintegration technique, is considered as an alternative. This method shows an improved performance near the resonance conditions both in the theoretical accuracy analysis and in the numerical tests.

The present study shows that higher order algorithms are more suitable than traditional Newmark methods, when a high accuracy is required near the resonance condition. Although higher order methods are more computationally expensive than traditional ones,

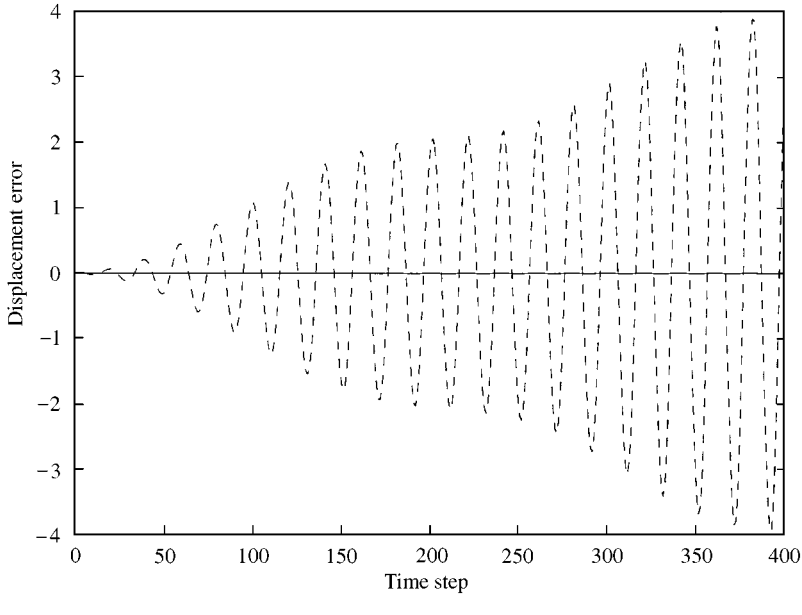

Figure 5. Displacement errors of the trapezoidal rule and PI3 — $\varepsilon = 0{\cdot}9$ — displacement: ____ higher order; _ _ _ _ trapezoidal rule.

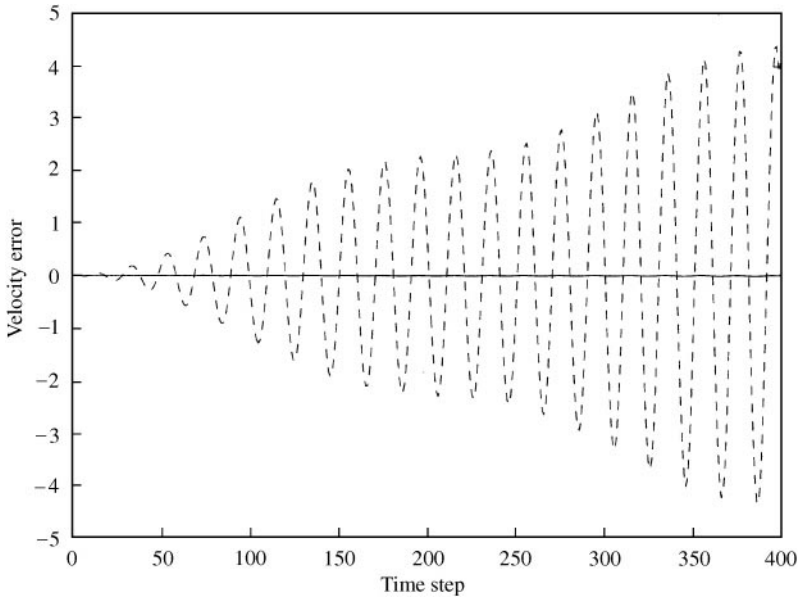

Figure 6. Velocity errors for the trapezoidal rule and PI3 — $\varepsilon = 0{\cdot}9$ — velocity: ____ higher order; - - - - trapezoidal rule.

effective implementation strategies are available (see, for example, the iterative solution procedure for a discontinuous Galerkin method described by Li and Wiberg [11]). Therefore, higher order algorithms appear to be a promising alternative to traditional second order methods.

REFERENCES

1. K. J. BATHE 1982 *Finite Element Procedures in Engineering Analysis*. Englewood Cliffs, NJ: Prentice-Hall.
2. T. J. R. HUGHES 1987 *The Finite Element Method. Linear Static and Dynamic Finite Element Analysis*. Englewood Cliffs, NJ: Prentice-Hall.
3. W. L. WOOD 1981 *International Journal of Numerical Methods in Engineering* **17**, 281–289. Numerical integration of structural dynamics equations including natural damping and periodic forcing terms.
4. W. L. WOOD 1990 *Practical Time-stepping Schemes*. Oxford: Clarendon Press.
5. S. N. PENRY and W. L. WOOD 1985 *International Journal of Numerical Methods in Engineering* **21**, 1941–1955. Comparison of some single-step methods for numerical solution of the structural dynamics equation.
6. A. PREUMONT 1982 *International Journal of Earthquake Engineering and Structural Dynamics* **10**, 691–697. Frequency domain analysis of time integration operators.
7. T. C. FUNG 1999 *International Journal of Numerical Methods in Engineering* **45**, 941–970. Weighting parameters for unconditionally stable higher-order accurate time step integration algorithms. Part 1 — First-order equations.
8. T. C. FUNG 1999 *International Journal of Numerical Methods in Engineering* **45**, 971–1006. Weighting parameters for unconditionally stable higher-order accurate time step integration algorithms. Part 2—Second-order equations.
9. J. LANGER, M. KLASZTORNY and S. EL-SAYED EL-BAGALATY 1992 *International Journal of Numerical Methods in Engineering* **33**, 889–905. Postintegration methods for numerical integration of non-linear dynamic equations of motion.
10. L. MEIROVITCH 1986 *Element of Vibration Analysis*. New York: McGraw-Hill.
11. X. D. LI and N.-E. WIBERG 1996 *International Journal of Numerical Methods in Engineering* **39**, 2131–2152. Structural dynamic analysis by a time-discontinuous Galerkin finite element method.